Trans Indian Inst Met
https://doi.org/10.1007/s12666-021-02380-w

ORIGINAL ARTICLE

Effect of Strain Rate and Measuring Temperature on Elastocaloric Effect and Multi-caloric Properties of $Co_{37.5}$ $Ni_{34.5}$ Al_{28} Paramagnetic Shape Memory Alloy

Muhammad Tahir Khan[1,2] · Qadeer Ul Hassan[3] · Liao Xiaoqi[4]

Received: 29 March 2021 / Accepted: 5 August 2021

Abstract In this study, the elastocaloric and magnetocaloric effects in a paramagnetic shape memory alloy, i.e., $Co_{37.5}$ $Ni_{34.5}$ Al_{28} alloy were investigated. The study reveals that the alloy shows an elastocaloric effect with a temperature change of 2.2 K under 400 Mpa keeping a strain rate of 0.25 s^{-1}. It shows a temperature change of over 1 K within a temperature span of 50 K including the room temperature. Under the same stress, with a strain rate of 0.50 s^{-1}, the material shows a temperature change of 2.7 K and gives more than 1 K temperature change within a span of 75 K including the ambient temperature. However, increasing the strain rate to 0.62 s^{-1} causes the material to break down. This shows that under a certain limit, the increase in the strain rate increases the elastocaloric temperature change and enhances the temperature window of the material along with the peak shifts toward lower measuring temperatures. Moreover, the study deduces that the material also exhibits a magnetocaloric effect. The study also reveals that both of the effects show temperature changes with the same sign and in the same region of the working temperature, thus enhancing one another.

Keywords Solid-state refrigeration · Elastocaloric effect · Magnetocaloric effect · Effect of strain rate · Multi-caloric

1 Introduction

In the recent times, energy crisis is a huge issue all over the world. The environmental impact of utilizing different types of energies is being investigated by many researchers. The use of conventional refrigeration system (CFCs) is not good for a healthy environment as it consumes a lot of energy [1–4]. Thus, solid-state refrigeration [5] is being explored as a solution to these issues. The Peltier effect is the only solid-state refrigeration method which can be used practically, however, it cannot produce the sufficient cooling needed for a larger application [6]. Thus, in the near future, the caloric effect-based cooling method is the most reliable solution for larger applications [7]. In caloric effect, heat is produced or absorbed in response to an external stimuli in specific materials [6]. This external stimuli can be either (1) electric [8], (2) magnetic field [9–11], (3) uniaxial stress [12–14], or (4) hydrostatic pressure [15]. For utilization of this technology in the real world, scientists have made efforts to get a material that is good in all aspects which are as follows: (a) huge temperature change (ΔT),(b) a good efficiency, (c) better fatigue life, and (d) a large temperature range of operation, etc. [16].

The refrigeration capability can be estimated by measuring its temperature change during the phase transition. The shape memory alloys (SMAs) have two phases, (1)

✉ Muhammad Tahir Khan
tahir_iiui14@yahoo.com

[1] MOE Key Laboratory for Nonequilibrium Synthesis and Modulation of Condensed Matter, State Key Laboratory for Mechanical Behavior of Materials, Xi'an Jiaotong University, Xi'an 710049, People's Republic of China

[2] Department of Physics, Riphah International University, Islamabad 38000, Pakistan

[3] School of Chemistry and Chemical Engineering, Shaanxi Normal University, Xi'an 710019, People's Republic of China

[4] College of Physics and Optoelectronic Engineering, Shenzhen University, Shenzhen 518060, People's Republic of China

Published online: 24 August 2021

low-temperature phase: martensite, and (2) high-temperature phase: austenite (high-temperature phase). The austenite phase has a more closely packed structure, having more entropy as compared to the martensite phase. The transformation of a material from austenite to martensite phase causes a reduction in the internal entropy and leaves a ΔT in the form of heat with an excessive entropy of the austenite phase. On the contrary, a decrease in the temperature can be seen in the material for the transformation from Martensite to Austenite phase, as it needs heat to increase its entropy [17]. This cycle of heat exclusion and inclusion, seen in the transformation between the two phases, can be used for the refrigeration. Similarly, magnetic SMAs [18, 19] show the same cycle of heat transfer during the magnetic phase change on Curie temperature. The paramagnetic state is a high-entropy state, while the ferromagnetic state is a low-entropy state. During a magnetic phase change, from paramagnetic to ferromagnetic, the material releases an excessive entropy in the form of heat while heat is required to randomize the magnetic domains. The martensitic (first order) phase change is dependent on an external stress, and the magnetic phase change is dependent on the external magnetic field [20, 21]. Thus, that the phase change temperature has can be modified by applying these external stimuli. NiTi [22]- and Cu [23]-based SMAs are some of the materials capable of showing high ΔT. An important factor which can effect the cooling efficiency of the material is the responding speed to the external stimuli. The influence of strain rate on the elastocaloric effect in different materials like on NiTi-based SMAs is being thoroughly investigated [24, 25].

In this study, the influence of different strain rates (0.25 s^{-1}, 0.50 s^{-1}, 0.62 s^{-1}) on different temperatures (243–323 K) for $Co_{37.5}$ $Ni_{34.5}$ $Al_{28.}$ is being investigated. Moreover, the combination of different calorics to get an enhanced ΔT is being proposed [26]. In this regard, the use of SMA, as it shows both elasto- and magnetic caloric effect, is proposed as the better approach [27]. For this, the two temperature changes on the same or nearly the same working temperature with the same sign, so that it can enhance each other and not cancel each other, are required [28, 29]. Many magnetic SMAs show both the elasto- and magnetocaloric effects but with opposite signs and hence cancel out each other [30]. There are only a few materials that show these effects with the same sign. The study investigates such multi-calorics for $Co_{37.5}$ $Ni_{34.5}$ $Al_{28.}$

2 Devices and Techniques

The polycrystalline alloy samples with the nominal compositions $Co_{37.5}$ $Ni_{34.5}$ Al_{28} were prepared. Corresponding ingots were fabricated by arc melting with 99.9% purity under argon atmosphere. The sample was annealed up to 1572 K for 24 h in evacuated quartz tubes and subsequently quenched into room temperature water. The martensitic transformation temperatures of the samples were determined by a differential scanning calorimetry (DSC, Q2000 from TA Instruments) with a temperature sweeping rate of 10 K/min. Its magnetic transition was characterized by measuring the magnetization versus temperature (M-T) curve under the magnetic field of 500 Oe Superconducting quantum interference device (SQUID, Model MPMS-3 from Quantum Design Inc.). The heat treated ingot was cut into the small square pillars with the size of 2.8 mm × 3 mm × 9 mm for stress–strain test and elastocaloric measurement, which were conducted in a testing machine (Autograph AG-I 50 kN Model M1, Shimadzu) with a compressive deformation mode. The machine compliance was taken care of during the compressive tests. Since it is generally accepted that the temperature change of elastocaloric effect ΔT_E provides more reliable and straightforward information to evaluate the elastocaloric performance of materials, the ΔT_E of the sample was detected directly by a T-type thermocouple welded on its surface. For ensuring adiabatic condition, we applied a high strain rate of 0.25%s^{-1} until 400 MPa was reached. This stress was kept loaded for 30 s to make sure that the sample came back to its original temperature and then unload with the same strain rate. We did the same experiment for the strain rates of 0.50%s^{-1} and 0.62%s^{-1}. The temperature change of magnetocaloric effect ΔT_M was also detected by a T-type thermocouple welded on the sample surface. To approximate the near adiabatic condition during ΔT_M measurement, the sample was rapidly placed into a chamber of 5 T magnetic field for 2 s and held for 50 s to wait for the sample to recover to its initial temperature. After that, the sample was quickly moved out from the chamber in 2 s for withdrawing the magnetic field to 0 T.

3 Results and Discussion

The heat treated ingot is cut into the small pieces, the transforming properties of alloy are revealed by the DSC and magnetic measurements in Fig. 1a. The blue line is for cooling and the red is for heating. The sample shows obvious latent heat peaks in its DSC curve upon heating/cooling cycle, which demonstrates that it undergoes martensitic transformation.

On cooling from high to low temperature, the martensitic transformation starting temperature M_s is 278 K and finishing temperature M_f is 253 K. Similarly, for heating process, the corresponding reverse transformation starting temperature A_s is 267 K and complete austenite phase is

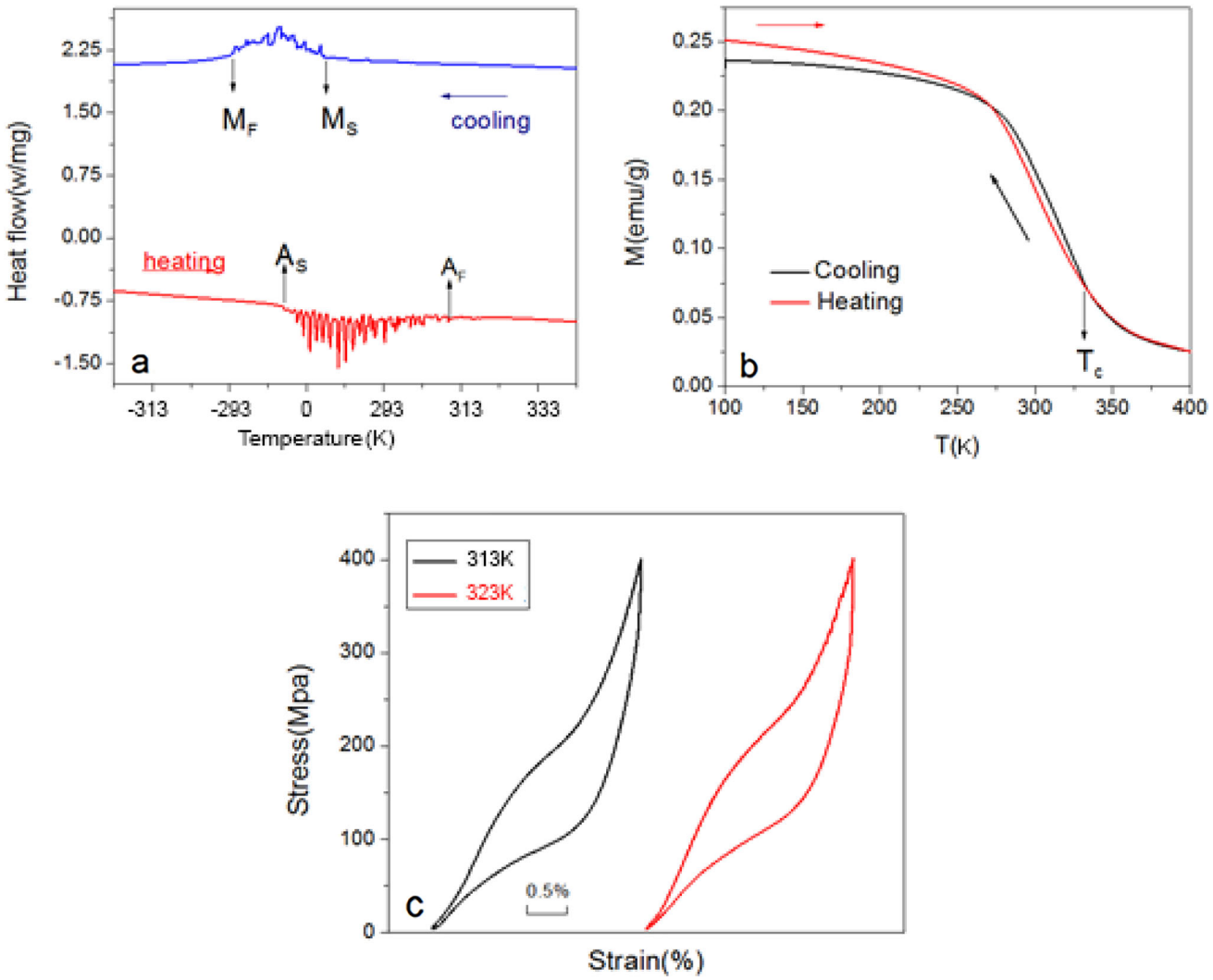

Fig. 1 **a** DSC curve for $Co_{37.5}$ $Ni_{34.5}$ Al_{28}, measured for both heating and cooling. **b** Magnetization versus temperature curve for $Co_{37.5}$ $Ni_{34.5}$ Al_{28} under the applied field of 500oe. **c** Stress–strain curve of $Co_{37.5}$ $Ni_{34.5}$ Al_{28} obtained at 313 K and 323 K with a maximum applied compressive stress of 400 MPa.

achieved at 310 K from the endothermic peak of the heating process.

The M–T curves measured under a magnetic field of 500 Oe for both cooling and heating processes are displayed in Fig. 1b. It shows that the magnetization increases at low temperature, demonstrating that the alloy undergoes a conventional ferromagnetic transition on cooling. The ferromagnetic transition temperature T_c is 330 K. Comparing with the cooling process, the ferromagnetic transition temperature is closer to the martensitic transformation temperature during the heating process Fig. 1b.

4 Stress–Strain Curve

For investigating the behavior of induced strain in the sample due to applied stress, we have plotted the stress versus strain curves on temperatures 313 K and 323 K which is just above A_f, with an applied stress of up to 400 MPa. The curve shows the typical features of its deformation behavior above A_f. As displayed in Fig. 1c, a complete superelastic behavior can be observed at these two testing temperatures upon loading up to 400 MPa, demonstrating that a complete stress-induced martensitic transformation can be achieved under 400 MPa.

5 Stress 400 Mpa Strain Rate 0.25 s^{-1}

We have applied a stress of 400 MPa with a strain rate of 0.25 s^{-1} on $Co_{37.5}$ $Ni_{34.5}$ Al_{28} and found change in temperature for a variety of temperatures. On 293 K, it shows max loading ΔT of 2.2 K, and for unloading, it is 1.89 K. This heat is actually obtained from phase change of martensite to austenite. As austenite is at the low-entropy state, the excessive disorderness of martensite come out in the form of heat. While unloading, it shows a negative peak in which heat is extracted from the sample. It is due to the austenite to martensite phase change. The data are combined in a "Temperature change of elastocaloric effect (ΔT_E) as a function of temperature for the loading and unloading process" as shown in Fig. 2b. The curves clearly shows that we get a highest ΔT in the vicinity of martensite phase change temperature. It is also noticeable that ΔT loading is larger than ΔT unloading because excessive heat is produced due to the movement of austenite/martensite phase boundaries and martensitic twin boundaries. This heat adds up while loading; while during unloading, as the sample needs heat and when some heat is already there, it will extract less heat from the environment; that is why the unloading curve shows comparatively less temperature change ΔT. The curve shows a ΔT of more than 1 K on the temperature span of 50 K (270 K–320 K) including room temperature.

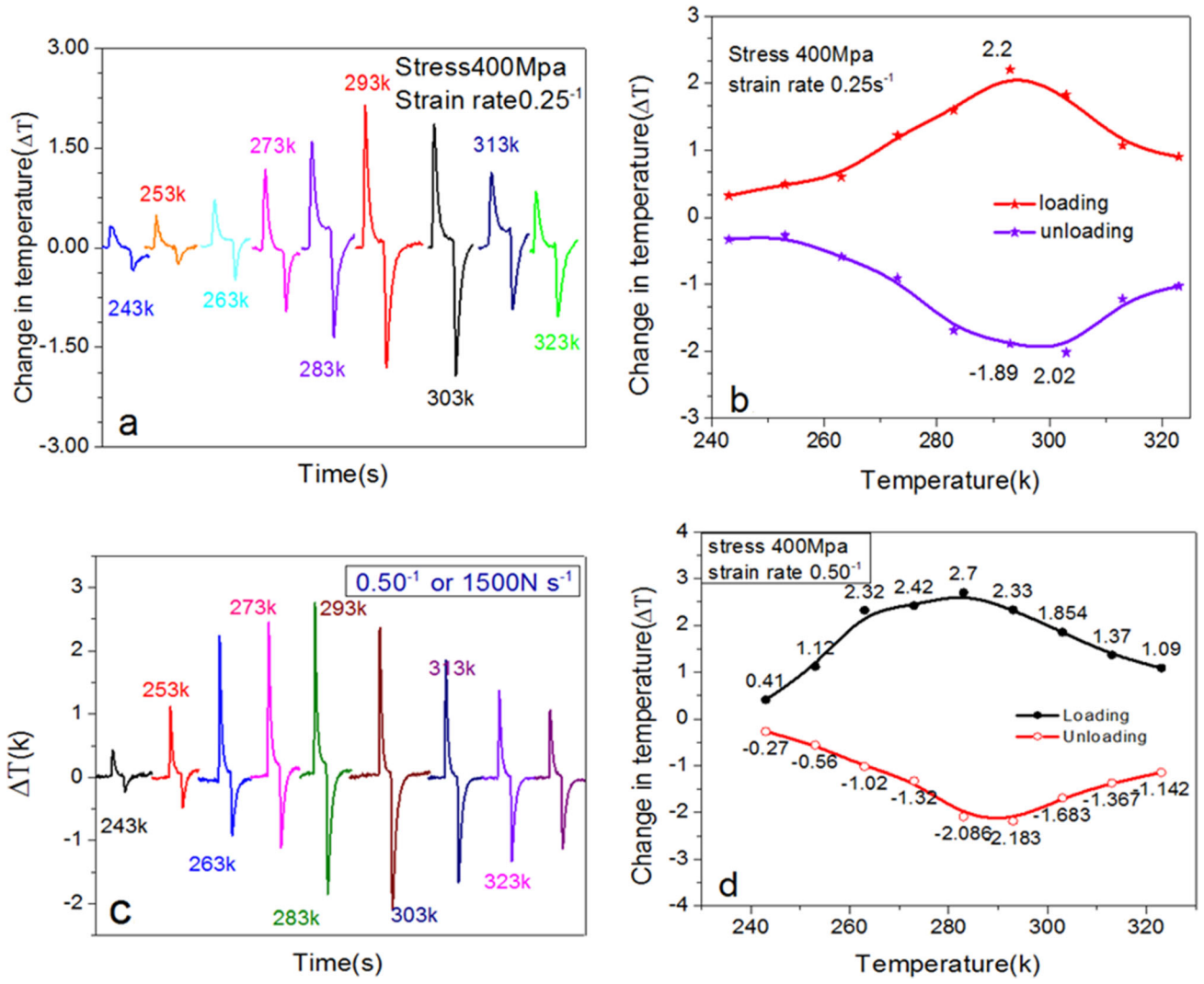

Fig. 2 **a** ΔT_E induced by stress of 400 Mpa with a strain rate of 0.25%s^{-1} on a series of working temperatures. **b** ΔT_E versus temperature with strain rate of 0.25%s^{-1} for loading and unloading. **c** ΔT_E of 400 Mpa with a strain rate of 0.50%s^{-1}. **d** ΔT_E versus temperature with strain rate of 0.50%s^{-1}.

6 Stress 400 Mpa Strain Rate 0.50 s^{-1}

Figure 2c shows a temperature versus change in temperature curve when a stress of 400 MPa is applied with a strain rate of 0.50 s^{-1}. The graph shows highest ΔT of 2.7 K on the temperature 283 K, while on unloading, we get 2.18 K at 293 K, and Fig. 2d shows a ΔT of 1 K on the temperature span of 75 K (250–325 K) including the room temperature. Further increasing the strain rate causes breakdown of the sample.

7 Effect of Strain Rate

Figure 3a shows comparison of the maximum temperature change in temperature curves for strain rate of 0.25 s^{-1} and 0.50 s^{-1}. We can notice there is a clear increase ΔT with increase in strain rate. Increasing strain rate from 0.25 s^{-1} (red curve) to 0.50 s^{-1}(black curve), the maximum ΔT increases from 2.2 K to 2.7 K during loading, similarly for unloading, it goes from − 1.89 K to − 2.086 K. An increased strain rate causes a better adiabatic condition and a higher isothermal entropy change. Similarly, increasing strain rate shifts the peak of the curve from 293 to 283 K. It means that the phase change temperature has shifted to lower value.

Figure 3b compares the ΔT of two curves while increasing the strain rate, ΔT increases on every temperature we tested. The temperature span ΔT also increases for 0.50 s^{-1} strain rate from 50 to 75 K (250 K-325 K) including room temperature.

The excessive fast loading and unloading (higher strain rates) can cause small microcracks in the sample. These microcracks propagate during every cycles and ultimately can damage the sample. Therefore, an appropriate limit of strain rate must be maintained to avoid break up or a huge reduction in sample fatigue life. In our study, when we increased the strain rate up to 0.62 s^{-1} the sample broke down. Moreover, normally, the change in temperature for loading is larger than that for unloading; this is because of the fact that during loading unloading process, it faces different types of fractions just like interfacial fraction of martensite and austenite, grain boundary or the interaction between phase interface. All these frictions cause excessive heat; during loading, heat is produced and the frictional heats are added positively to the peak; while during unloading, heat is absorbed and the frictional heat produced inside diminishes the absorption of heat which results in a relative small peak as compared to the loading peak.

8 Magnetocaloric Effect

The magnetocaloric effect is also characterized by detecting its ΔT_M. The ΔT_M for applying and withdrawing 5 T magnetic field has been determined from the time dependence of ΔT, as exemplified by the curve at 283 K (Fig. 3b). The change in temperature in magnetocaloric effect ΔT_M on different temperatures with external field of 5 T can be seen in Fig. 4a. The temperature dependence of ΔT_M changes slightly with temperature forming small peak

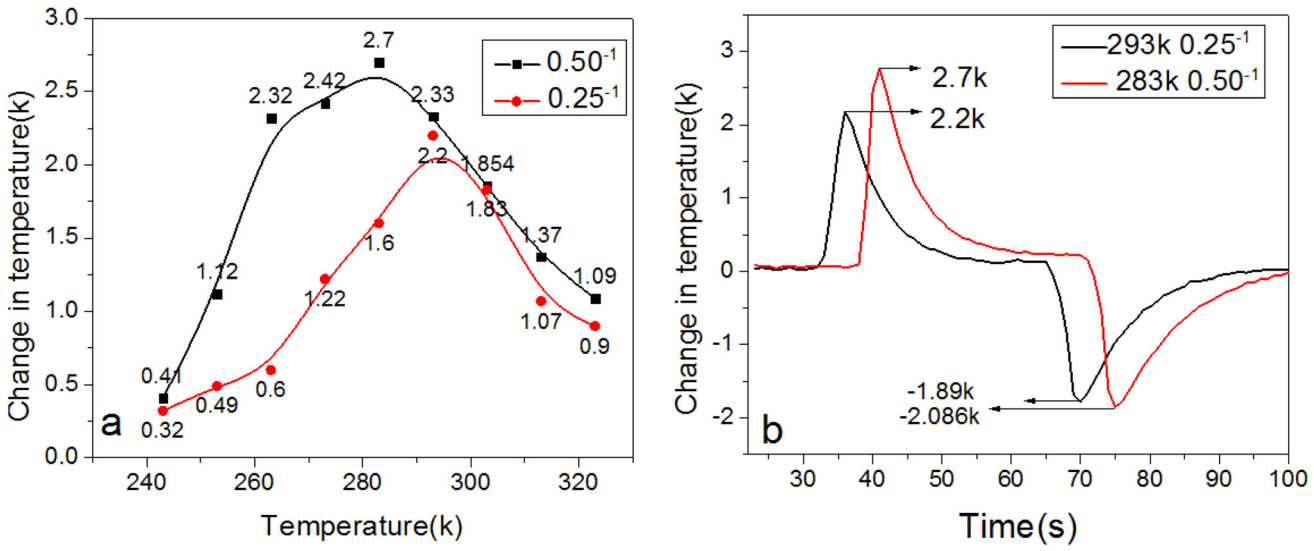

Fig. 3 **a** Comparison of T versus ΔT curves of strain rates 0.25 s^{-1} (lower curve) and 0.50 s^{-1} (upper curve). **b** Comparison of maximum ΔT of elastocaloric effect at strain rate of 0.25 s^{-1} (lower curve) and 0.50 s^{-1} (upper curve).

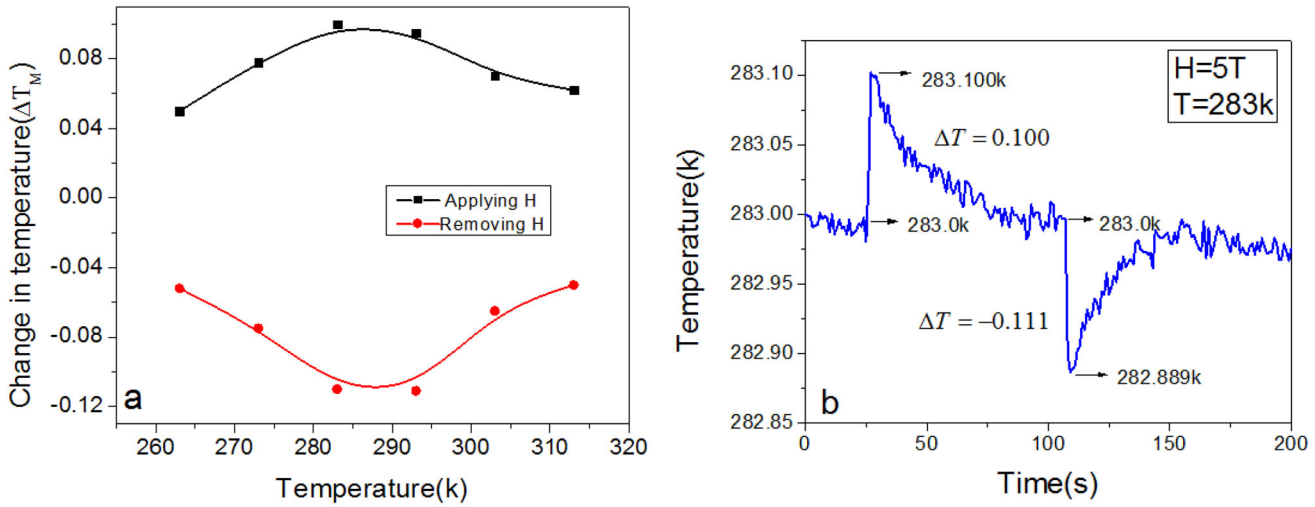

Fig. 4 **a** ΔT_M as a function of temperature with applied magnetic field of 5 T. **b** Maximum ΔT_M curve with applied field of 5 T which occurred at 283 K.

within the ferromagnetic transition range for applying and withdrawing magnetic field processes.

9 Multi-Caloric

Figure 5 summarizes both the elastocaloric effect (red curve) and magnetocaloric effect (blue curve). Both the ΔT_E and ΔT_M have the same sign, and most importantly, peaks of both the curves are very close to each other which means that both ΔT_E and ΔT_M will enhance each other when 400 MPa stress and 5 T external magnetic field are applied simultaneously on $Co_{37.5}$ $Ni_{34.5}$ Al_{28}. This combination of caloric properties is very important to enhance the capacity of this material in the field of solid-state refrigeration. Moreover, it is clear that ΔT_E is dominant on ΔT_M, which shows that the vibrational entropy change is much more dominant on the magnetic entropy change.

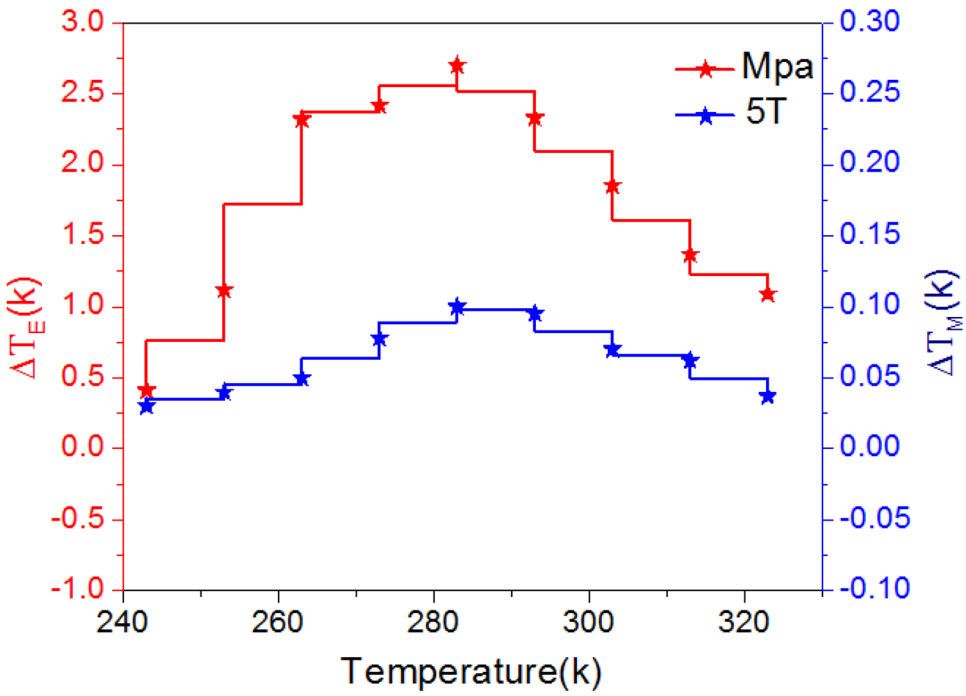

Fig. 5 ΔT as a function of temperature for magnetocaloric effect (lower curve, right scale) and for elastocaloric effect (upper curve, left scale)

10 Conclusion

In conclusion, the elastocaloric and magnetocaloric effects of alloy have been studied. In our work, we have checked the strain rate effect on the elastocaloric effect ΔT_E, and as compared to 0.25 s^{-1}, the 0.50 s^{-1} strain rate shows larger ΔT_M on different temperatures. With increase in strain rate, the performance of the caloric properties in the material increases. It shows a maximum ΔT_E of 2.7 K with a worthy value of more than 1 K in a temperature window of 75 K including the ambient temperature. The important finding is that, the sample has maximum ability to withhold a strain rate of 0.50 s^{-1} for a stress of 400 MPa, as further increase in the strain rate results in the breakdown of the sample. $Co_{37.5}$ $Ni_{34.5}$ Al_{28} shows both elasto- and magnetocaloric effects. Moreover, ΔT_E and ΔT_M have the same sign and peaks in the same region of working temperature. These capabilities make this material a good candidate for solid-state refrigeration in the near future.

Acknowledgements The present work was financially supported by National Natural Science Foundation of China (Grant Nos. 51471127, 51431007 and 51371134), Program for Young Scientific New-star in Shaanxi Province of China (No. 2014KJXX-35), the Fundamental Research Funds for Central Universities of China.

Author Contributions † M.T and Q.-U.H. have contributed equally to this work and should be considered as co-first authors.

References

[1] Chauhan A et al. *MRS Energy & Sustainability* 2 (2015).
[2] Houghton J T, Ding Y, Griggs D J, Noguer M, van der Linden P J, Dai X, Maskell K, and Johnson C *Climate Change 2001: The Scientific Basis*, (Vol 881), Cambridge University Press, Cambridge (2001).
[3] Root T L, Price J T, Hall K R, Schneider S H, Rosenzweig C, and Pounds J A, *Nature* **421** (2003) 57.
[4] Mendelsohn R, Nordhaus W D, Shaw D, *Am. Econ. Rev.* (1994) 753.
[5] Dingquan X, *Ferroelectrics* **231** (1999) 133.
[6] Manosa L, Planes A, and Acet M, *J. Mater. Chem. A* **1** (2013) 4925.
[7] Liu J, Gottschall T, Skokov K P, Moore J D, and Gutfleisch O, *Nat. Mater.* **11** (2012) 620.
[8] V.K. Pecharsky, K.A. Gschneidner Jr., Phys. Rev. Lett. 78 (23) (1997) 4494.
[9] Brück E, lyn M, Tishin A M, and Tegus O J, *Magn.Magn. Mater.* **290–291** (2005) 8.
[10] Moya X, Stern-Taulats E, Crossley S, González-Alonso D, Kar-Narayan S, Planes A, Mañosa L, and Mathur N D, *Adv. Mater.* **25** (2013) 1360.
[11] Manosa L, González-Alonso D, Planes A, Barrio M, Tamarit, J -L, Titov I S, Acet M, Bhattacharyya A, and Majumdar S, *Nat. Commun.* **2** (2011) 595.
[12] Bechtold C, Chluba C, Lima de Miranda R, and Quandt E, *Appl. Phys. Lett.* **101** (2012) 091903.
[13] Xiao F, Fukuda T, and Kakeshita T, *Appl. Phys. Lett.* **102**(2013) 161914.
[14] Xiao F, Fukuda T, Kakeshita T, and Jin X, *Acta Mater.* **87** (2015) 8.
[15] Khan M T, Wang Y, Wang C, Liao X, Yang S, Song X, and Ren X, *Scripta Materialia* **146** (2018) 182.
[16] Fähler S et al. *Adv. Eng. Mater.* **14** (2012) 10.
[17] Mañosa L, and Planes A, *Philos. Trans. Royal Soc. A Math. Phys. Eng. Sci.* **374** (2016) 20150310.
[18] Manosa L, and Planes A, *Adv. Mater.* **29** (2017) 1.
[19] Hu Y, Li Z, Yang B, Qian S, Gan W, Gong Y, and Zhao X, *APL Mater.* **5** (2017) 046103.
[20] Krenke T, Duman E, Acet M, Wassermann E F, Moya X, Mañosa L, and Planes A, *Nat. Mater.* **4** (2005) 450.
[21] Xu S, Huang H -Y, Xie J, Takekawa S, Xu X, Omori T, and Kainuma R, *APL Mater.* **4** (2016) 106106
[22] Xiao F, Fukuda T, and Kakeshita T, *Scripta Mater.* **124** (2016) 133.
[23] Singal H C, Mahajan A, and Singh R, *Int. J. Mech. Eng.* **3** (2016) 46.
[24] Emsley J, *Nature's Building Blocks*, Oxford University Press, Oxford (2001).
[25] Hu , Li Z, Yang B, Qian S, Gan W, Gong Y, Li Y, Zhao D, Liu J, Zhao X, Zuo L, Wang D, and Du Y, *APL Mater.* **5** (2017) 046103.
[26] Nikam A N, and Hole J A, **2** (2014) 6.
[27] Cui J, Wu Y, Muehlbauer J, Hwang Y, Radermacher R, Fackler S, Wuttig M and Takeuchi I, *Appl. Phys. Lett.* **101** (2012) 1175.
[28] Xu S, Huang H Y, Xie J, Takekawa S, Xu X, Omori T, and Kainuma R, *APL Mater.* **4** (2016) 106106.
[29] Ossmer H, Miyazaki S, and Kohl M, *Mater. Today Proc.* **2** (2015) S971–S974.
[30] Ossmer H, Lambrecht F, Gültig M, Chluba C, Quandt E and Kohl M, *Acta Mater.* **81** (2014) 9.